

18-F fluorodeoxyglucose uptake in positron emission tomography as a pathological grade predictor for renal clear cell carcinomas

Yoshifumi Noda · Masayuki Kanematsu · Satoshi Goshima · Natsuko Suzui · Yoshinobu Hirose · Kengo Matsunaga · Hironori Nishibori · Hiroshi Kondo · Haruo Watanabe · Hiroshi Kawada · Nobuyuki Kawai · Yukichi Tanahashi · Kyongtae T. Bae

Received: 22 July 2014 / Revised: 23 December 2014 / Accepted: 20 February 2015 / Published online: 9 April 2015
© European Society of Radiology 2015

Abstract

Objectives To evaluate the usefulness of Fluorine-18 fluorodeoxyglucose positron emission tomography/computed tomography (18-F FDG-PET/CT) in the prediction of Fuhrman pathological grades of renal clear cell carcinoma (cRCC).

Methods This retrospective study was approved by our institutional review board, and written informed consent was waived. Thirty-one patients with pathologically proven cRCC underwent 18-F FDG-PET/CT for tumour staging. Maximum

standardized uptake value of cRCC (tumour SUV_{max}) and mean SUV of the liver and spleen (liver and spleen SUV_{mean}) were measured by two independent observers. Tumour SUV_{max} , tumour-to-liver SUV ratio, and tumour-to-spleen SUV ratio were correlated with the pathological grades.

Results Logistic analysis demonstrated that only the tumour-to-liver SUV ratio was a significant parameter for differentiating high-grade (Fuhrman grades 3 and 4) tumours from low-grade (Fuhrman grades 1 and 2) tumours ($P=0.007$ and 0.010 for observers 1 and 2, respectively). Sensitivity, specificity, and positive and negative predictive values for detecting tumours of Fuhrman grades 3 and 4 were 64, 100, 100, and 77 %, respectively, for observer 1, and 79, 88, 85, and 83 %, respectively, for observer 2. **Conclusions** The tumour-to-liver SUV ratio with 18-F FDG-PET/CT appeared to be a valuable imaging biomarker in the prediction of high-grade cRCC.

Key Points

- Tumour SUV_{max} was correlated with the Fuhrman grades.
- High-grade tumours have significantly higher SUV_{max} than low-grade tumours.
- Tumour-to-liver SUV ratio is useful in the prediction of high-grade cRCC.

Y. Noda · M. Kanematsu (✉) · S. Goshima · H. Kondo · H. Watanabe · H. Kawada · N. Kawai · Y. Tanahashi
Department of Radiology, Gifu University Hospital, 1-1 Yanagido, Gifu 501-1194, Japan
e-mail: masa_gif@yahoo.co.jp

M. Kanematsu
Department of Radiology Services, Gifu University Hospital, 1-1 Yanagido, Gifu 501-1194, Japan

N. Suzui
Department of Pathology, Gifu University Hospital, 1-1 Yanagido, Gifu 501-1194, Japan

Y. Hirose
Department of Pathology, Osaka Medical College, Osaka, Japan

K. Matsunaga
Department of Pathology, Kizawa Memorial Hospital, Minokamo, Japan

H. Nishibori
Department of Radiology, Kizawa Memorial Hospital, Minokamo, Japan

K. T. Bae
Department of Radiology, University of Pittsburgh Medical Center, Pittsburgh, PA, USA

Keywords Positron emission tomography · Renal clear cell carcinoma · Fuhrman grade · Tumour-to-liver SUV ratio · Imaging

Introduction

Renal cell carcinoma (RCC), the main solid cancer of the kidney, is the sixth most common cancer in men and eighth most common in women in the United States [1]. Annually, 64,770 patients are diagnosed with RCC, and 13,570 die as a

result of the disease [1]. Renal clear cell carcinoma (cRCC) is the most common histological subtype, accounting for approximately 75 % of all RCCs [2, 3]. RCCs are often incidentally detected in asymptomatic individuals as a result of the widespread use of computed tomography (CT), magnetic resonance imaging (MRI), and ultrasound (US) [4, 5]. Given the metastatic potential of RCC, it is crucial to efficiently and accurately stage RCC once it is detected in order to determine the best therapeutic strategies for patients.

Fluorine-18 fluorodeoxyglucose (18-F FDG)-positron emission tomography (PET) is widely used in workups for malignancy, including the detection, differential diagnosis, staging and/or restaging, therapeutic decision-making, follow-up, and prognosis of most malignancies [6, 7]. The detectability of 18-F FDG-PET/CT in malignant tumours depends on the degree of 18-F FDG uptake in tumours relative to that in the surrounding normal tissues. Generally, cancer cells exhibit increased glucose transporter (GLUT) expression [8] as well as higher levels of hexokinase and phosphofructokinase activity that promotes glycolysis [9]. This results in increased glucose uptake across cancer cell membranes and/or increased glycolytic rates in cancer cells, and the subsequent increase in 18-F FDG uptake seen in tumours.

The role of 18-F FDG-PET/CT in the diagnosis of urologic oncology remains uncertain. The physiological excretion of 18-F FDG through the kidneys makes it difficult to visualize the structures and tumours against the high background of 18-F FDG accumulation. Moreover, it is known that RCC consists of glycogen-rich cells and that the cancer cell itself has a low potential for metabolizing glucose, frequently resulting in no or minimal uptake of 18-F FDG [10]. Nevertheless, according to previous reports, sensitivity and specificity of 18-F FDG PET in the diagnosis of RCC has ranged from 47 to 94 % and from 80 to 100 %, respectively [11–13].

In our clinical practice, we have found that high-grade cRCC often shows increased 18-F FDG uptake. Previous reports have described a significant difference in disease-specific survival rates between patients with high- and low-grade tumours [14–18]. Predicting tumour grade may be of value in the treatment and management of patients with cRCC. Our literature search did not unearth any previous reports on the relationship between 18-F FDG uptake and pathological grades of cRCC. Thus, the purpose of this study was to evaluate the usefulness of 18-F FDG PET/CT in the prediction of Fuhrman pathological grades of cRCC.

Materials and methods

Patients

This retrospective study was approved by our institutional review board, and written informed consent was waived.

Between August 2008 and November 2013, 34 consecutive patients with pathologically proven cRCC underwent 18-F FDG-PET/CT imaging for preoperative tumour staging. Three of the 34 patients were excluded from our study cohort because the interval between 18-F FDG-PET/CT imaging and pathological diagnosis was over 3 months. Thus, the remaining 31 patients (mean age, 64.5 ± 13.7 years; range, 36–81 years), including 19 men (mean age, 60.3 ± 14.8 years; range, 36–81 years) and 12 women (mean age, 71.1 ± 8.8 years; range, 53–79 years), comprised our study cohort. The interval between the pathological diagnosis and following PET/CT ranged from 3 to 76 days (mean 28.4 ± 18.1 days).

18-F FDG-PET/CT imaging

Patients were instructed to fast for at least 5 hours prior to 18-F FDG-PET/CT acquisition. Blood glucose levels were measured before imaging, and were lower than 200 mg/dl in all patients. All imaging was performed with a 16-section PET/CT system (Biograph Sensation 16; Siemens Medical Solutions, Erlangen, Germany), which comprised a 16-section high-performance multi-detector low-dose CT system with a lutetium oxyorthosilicate-based PET system. Sixty minutes after the administration of 18-F FDG (mean, 3.4 ± 0.6 MBq/kg; range, 2.4–4.7 MBq/kg), whole-body CT was initially performed, primarily for attenuation correction, with patients holding their breath in mid-expiration phase, and included an area from the vertex to the pelvis. The parameters were as follows: section width, 5 mm; table feed per rotation, 18 mm; rotation time, 0.5 s; tube voltage, 120 kVp; quality reference mAs, 100 mAs in CARE Dose 4D (Siemens Medical Solutions); and field of view, 70 cm. Images of eight bed position (16.2-cm axial field of view), 2 min each, were acquired. Attenuation-corrected PET images were reconstructed from the CT data using a 3-D ordered subset expectation maximization algorithm (eight subsets, three iterations).

PET image analysis

Two nuclear medicine physicians (H.W. and H.K., with 7 and 5 years of experience in the interpretation of PET images, respectively), who were blinded to patient clinical information, retrospectively reviewed all 18-F FDG-PET/CT images on a commercially available dedicated DICOM (Digital Imaging and Communications in Medicine) viewer. The nuclear medicine physicians measured the maximum standardized uptake value of cRCC (tumour SUV_{max}) by drawing a region of interest (ROI) encompassing as much of the tumour area as possible. The tumour SUV_{max} was measured on axial, sagittal, and coronal images, and then averaged. Care was taken to exclude measurements from regions of physiological excretion in the renal collecting system. Further, an elliptical ROI was drawn to encompass as much of the right hepatic lobe as possible on the

Table 1 Patient Background Factors and Findings at Histopathology

	High-grade cRCC (<i>n</i> =14)	Low-grade cRCC (<i>n</i> =17)
Patient age	63.2±13.3 (41–81)	65.5±14.4 (36–79)
Male-to-female	9:5	10:7
Tumor size (mm)	79.7±31.0 (35–152)	57.2±30.4 (26–129)
Fuhrman grade (<i>n</i> =31)		
1	–	2 (6 %)
2	–	15 (48 %)
3	13 (42 %)	–
4	1 (4 %)	–

Note: Patient age and tumor size are means ± 1 standard deviation, with ranges in parentheses.

axial images in order to measure the mean SUV (SUV_{mean}) of the liver. Likewise, the SUV_{mean} of the spleen was measured. Tumour-to-liver SUV and tumour-to-spleen SUV ratios were calculated as ratios of the tumour SUV_{max} to the SUV_{mean} of the liver and spleen, respectively.

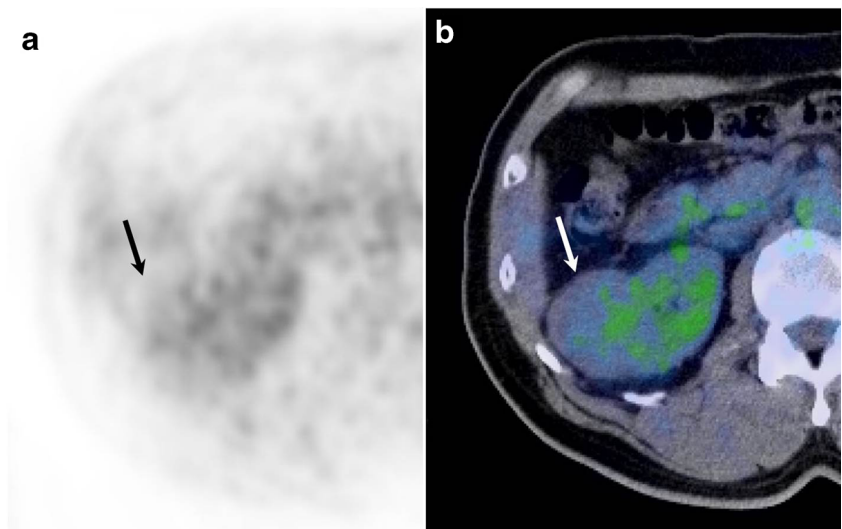
Standard of reference

An experienced pathologist (N.S., with 15 years of experience in tumour pathology), who was blinded to clinical or radiological information, microscopically evaluated haematoxylin/eosin stained specimens of surgically resected cRCCs in order to determine their Fuhrman grades (14).

Statistical analysis

Statistical analyses were performed using MedCalc for Windows, version 13.1.1 (MedCalc Software, Ostend, Belgium). Since survival rates for patients with Fuhrman grade 1 and 2 cRCCs are significantly better than for those with grade 3 and 4 tumours [19], our patients were divided into two categories:

Fig. 1 Axial slices of (a) F-18 positron emission tomography and (b) fused-image PET/CT in a 57-year-old man show low F-18 FDG uptake (tumour SUV_{max} of 2.86) in a 46-mm right renal mass proven to be a Fuhrman grade 2 cRCC



low-grade (Fuhrman grade 1/2) and high-grade tumours (Fuhrman grade 3/4). Patient age, tumour size, and gender were compared between the two categories using the Mann–Whitney *U* and chi-square tests. Regression analysis was performed to evaluate the correlation between tumour SUV_{max} and tumour size. Logistic regression analysis was performed for the discrimination of high-grade tumours using the following parameters: tumour size, tumour SUV_{max} , tumour-to-liver SUV ratio, and tumour-to-spleen SUV ratio. In logistic regression analysis, all parameters were analyzed simultaneously, and the interaction terms were considered. One-way analysis of variance (ANOVA) was used to evaluate differences between Fuhrman grades. The Mann–Whitney *U* test was conducted to evaluate differences between the two categories. The intraclass correlation coefficient was calculated for each of the observer measurements in order to evaluate interobserver differences for significance. A *P* value less than 0.05 was considered significant.

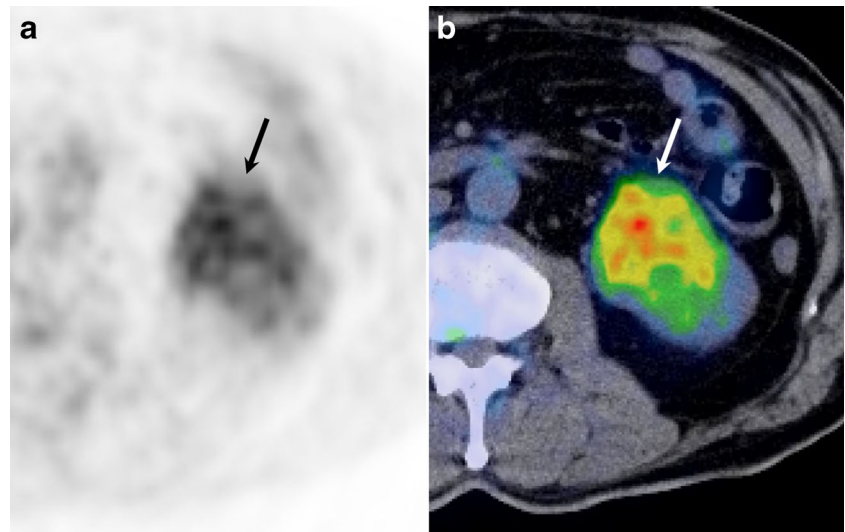
An optimal cutoff value based on maximum sensitivity and specificity was identified for the detection of Fuhrman grade 3/4 tumours with the highest area under the receiver operating characteristic (ROC) curve. ROC curves were fitted to the cutoff value to compute the sensitivity, specificity, positive and negative predictive values, and area under the ROC curve (AUC) for Fuhrman grade 3/4 tumour detection. AUCs for tumour SUV_{max} , tumour-to-liver SUV ratio, and tumour-to-spleen SUV ratio were compared using the Hanley and McNeil method [20].

Results

Patient background factors and tumour characteristics

Patient background factors and Fuhrman grades of the 31 cRCCs in 31 patients are summarized in Table 1. No

Fig. 2 Axial slices of (a) F-18 positron emission tomography and (b) fused-image PET/CT in a 60-year-old man show high F-18 FDG uptake (tumour SUV_{max} of 6.12) in a 52-mm left renal mass pathologically proven to be a Fuhrman grade 3 cRCC



significant difference was found in patient age ($P=0.69$) or gender ($P=0.95$) between the high- and low-grade tumours. Of the 31 patients, two had a Fuhrman grade 1 tumour, 15 had a grade 2, 13 had a grade 3, and one had a grade 4 tumour. PET/CT images of Fuhrman grade 2 and 3 cRCCs are illustrated in Figs. 1 and 2, respectively. The maximum cRCC diameter ranged from 26 to 152 mm, with a mean size of 67.4 ± 32.3 mm. The maximum diameter of the high-grade tumours (range 35–152 mm, mean 79.7 ± 31.0 mm) was greater than that of the low-grade tumours (range 26–129 mm, mean 57.2 ± 30.4 mm) ($P=0.02$) (Fig. 3).

Correlation between tumour SUV_{max} and tumour size

The tumour SUV_{max} (range 1.8–20.7 and mean 5.0 ± 3.7 vs. range 1.8–19.0 and mean 4.5 ± 3.2 for observers 1 and 2,

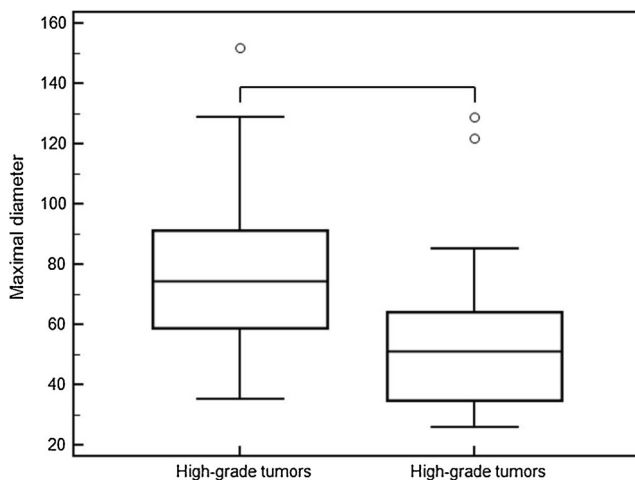


Fig. 3 Box plot showing the maximum diameter of cRCC. The maximum diameter of the high-grade tumours was greater than that of the low-grade tumours ($P=0.02$)

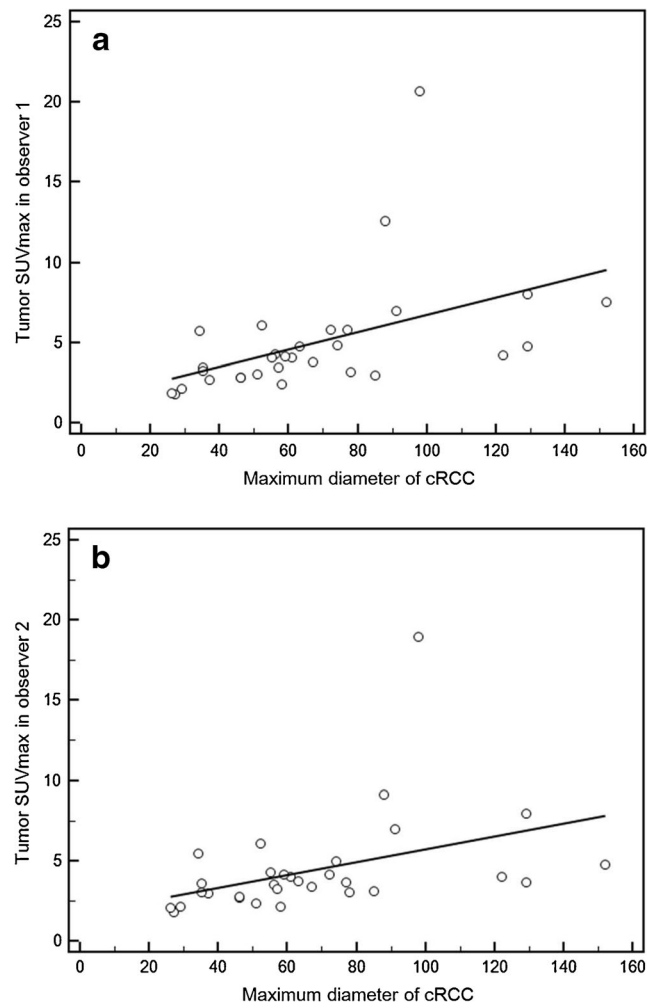


Fig. 4 Scatter plots showing correlation between the tumour SUV_{max} and tumour size for observers 1 (a) and 2 (b). There was a moderate correlation between tumour SUV_{max} and tumour size ($r=0.47$, $P=0.0066$ and $r=0.40$, $P=0.024$, respectively)

Table 2 Tumor SUV_{max}, Tumor-to-Liver SUV Ratio, and Tumor-to-Spleen SUV Ratio for cRCC of Different Fuhrman Grades

	Observer 1	Observer 2	ICC
Tumor SUV _{max}			
Grade 1 (n=2)	3.52±0.9 (2.85–4.19)	3.37±0.9 (2.74–4.00)	–
Grade 2 (n=15)	3.35±1.2 (1.81–5.74)	3.14±1.1 (1.81–5.46)	0.92
Grade 3 (n=13)	6.93±4.9 (3.19–20.71)	5.93±4.3 (3.06–19.0)	0.94
Grade 4 (n=1)	6.97	6.99	-
Tumor-to-liver SUV ratio			
Grade 1 (n=2)	1.49±0.4 (1.20–1.79)	1.37±0.1 (1.30–1.44)	–
Grade 2 (n=15)	1.47±0.6 (0.72–2.54)	1.40±0.5 (0.76–2.42)	0.92
Grade 3 (n=13)	3.03±1.9 (1.22–7.93)*	2.98±0.6 (1.34–8.87)*	0.92
Grade 4 (n=1)	3.07	3.21	–
Tumor-to-spleen SUV ratio			
Grade 1 (n=2)	1.77±0.2 (1.62–1.91)	1.58±0.3 (1.39–1.77)	–
Grade 2 (n=15)	1.83±0.6 (0.87–2.84)	1.92±0.7 (0.91–3.87)	0.78
Grade 3 (n=13)	3.82±2.2 (1.58–9.82)*	3.16±2.0 (1.64–8.95)*	0.80
Grade 4 (n=1)	3.77	4.34	-

Note: Data are means ± 1 standard deviation, with ranges in parentheses. cRCC renal clear cell carcinoma, ICC intraclass correlation coefficient between two observers
*Value was significantly greater than that with Fuhrman grade 2.

respectively) was moderately correlated with tumour size ($r=0.47$, $P=0.0066$ vs. $r=0.40$, $P=0.024$ for observers 1 and 2, respectively) (Fig. 4).

Correlation between SUV and pathological grade

Logistic regression analysis demonstrated that only the tumour-to-liver SUV ratio was a significant parameter for differentiating high-grade from low-grade tumours ($P=0.007$ and 0.010 for observers 1 and 2, respectively). The mean tumour SUV_{max}, tumour-to-liver SUV ratio, and tumour-to-spleen SUV ratio are summarized in Tables 2 and 3. The mean tumour-to-liver and tumour-to-spleen SUV ratios were

significantly higher for Fuhrman grade 3 compared to grade 2 tumours ($P<0.05$). Intraclass correlation coefficients demonstrated substantial to almost perfect agreement between the measurements by the two observers (Table 2). The mean tumour SUV_{max}, tumour-to-liver SUV ratio, and tumour-to-spleen SUV ratio for the high-grade tumours were greater than those for the low-grade tumours ($P=0.0004–0.0029$) (Figs. 5, 6 and 7). Interobserver reproducibility was excellent for tumour SUV_{max}, tumour-to-liver SUV ratio, and tumour-to-spleen SUV ratio (intraclass correlation coefficient, 0.78–0.98) (Table 3).

The AUCs for tumour-to-liver SUV ratio (0.82 and 0.83 for observers 1 and 2, respectively) tended to be higher than those

Table 3 Liver SUV_{mean}, Spleen SUV_{mean}, Tumor SUV_{max}, Tumor-to-Liver SUV Ratio, and Tumor-to-Spleen SUV Ratio of the High and Low Pathological Grade Groups

Parameter	Observer 1			Observer 2			Observer 1 vs. 2	
	High-grade cRCC (n=14)	Low-grade cRCC (n=17)	P value	High-grade cRCC (n=14)	Low-grade cRCC (n=17)	P value	ICC for high-grade cRCC	ICC for low-grade cRCC
Liver SUV _{mean}	2.31±0.5 (1.47-2.97)	2.36±0.5 (1.89-3.97)	0.80	2.08±0.5 (1.38-2.79)	2.36±0.1 (1.90-4.09)	0.28	0.89	0.94
Spleen SUV _{mean}	1.80±0.4 (1.14-2.40)	1.87±0.1 (1.38-2.51)	0.26	1.74±0.4 (0.85-2.41)	1.84±0.1 (1.28-2.33)	0.50	0.92	0.70
Tumor SUV _{max}	6.94±4.7 (3.19-20.71)	3.37±0.3 (1.81-5.74)	0.0006*	6.01±4.2 (3.06-18.98)	3.17±1.0 (1.81-5.46)	0.0009*	0.98	0.92
Tumor-to-Liver SUV ratio	3.04±1.8 (1.22-7.93)	1.47±0.1 (0.72-2.54)	0.0011*	2.99±2.0 (1.34-8.87)	1.39±0.5 (0.76-2.42)	0.0004*	0.96	0.90
Tumor-to-Spleen SUV ratio	3.82±2.1 (1.58-9.82)	1.83±0.1 (0.87-2.84)	0.0003*	3.24±1.9 (1.64-8.95)	1.88±0.2 (0.91-3.87)	0.0029*	0.91	0.78

Note: Data are means ± 1 standard deviation, with ranges in parentheses. cRCC renal clear cell carcinoma, ICC intraclass correlation coefficient between observers

* $P<0.05$, significant difference

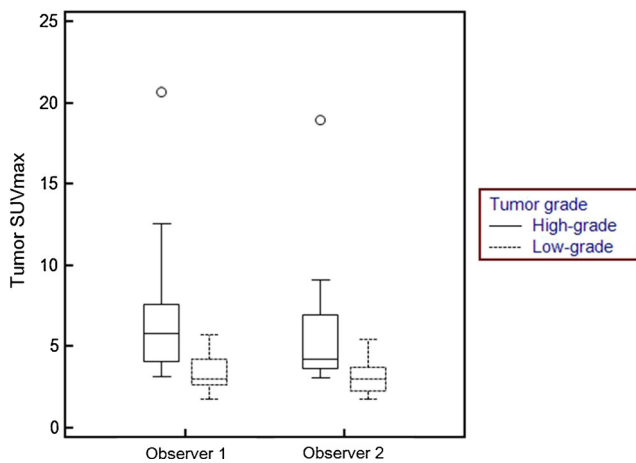


Fig. 5 Box plot showing the tumour SUV_{max} for observers 1 and 2. The mean tumour SUV_{max} of the high-grade tumours was greater than that of the low-grade tumours ($P=0.0006$ in observer 1, and $P=0.0009$ in observer 2)

for tumour SUV_{max} (0.76 and 0.76 for observers 1 and 2, respectively) and tumour-to-spleen SUV ratio (0.80 and 0.75 for observers 1 and 2, respectively); however, no significant difference was found between these indices ($P=0.40$ – 0.99). On the basis of the ROC analysis, the cutoff values for tumour SUV_{max}, tumour-to-liver SUV ratio, and tumour-to-spleen SUV ratio for differentiating between high- and low-grade tumours were 3.46 and 3.28, 2.54 and 1.80, and 2.60 and 1.90 for observers 1 and 2, respectively. In differentiating high- from low-grade tumours, observer 1 used a cutoff value of 2.54 for the tumour-to-liver SUV ratio, and observer 2 used a cutoff value of 1.80. This yielded sensitivity, specificity, and positive and negative predictive values of 64, 100, 100, and 77 % for observer 1, and 79, 88, 85, and 83 % for observer 2, respectively (Table 4).

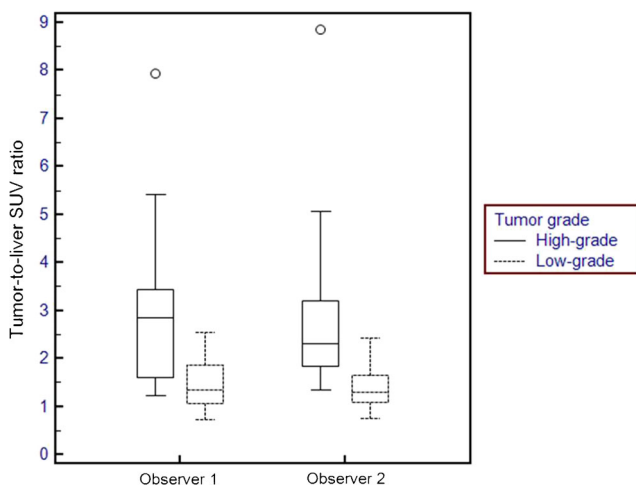


Fig. 6 Box plot showing the tumour-to-liver SUV ratio for observers 1 and 2. The mean tumour-to-liver SUV ratio of the high-grade tumours was greater than that of the low-grade tumours ($P=0.0011$ in observer 1, and $P=0.0004$ in observer 2)

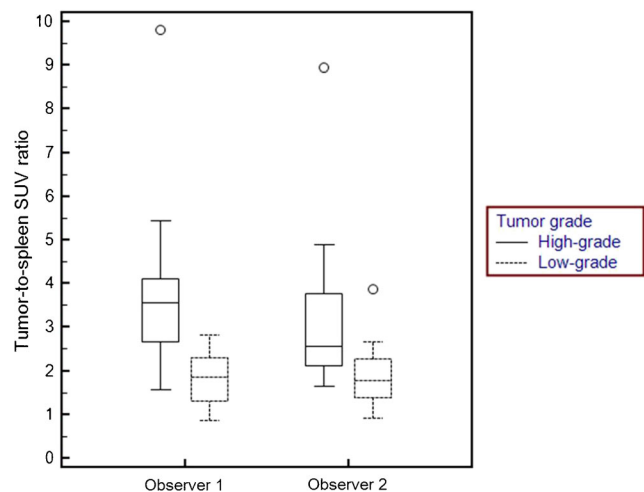


Fig. 7 Box plot showing the tumour-to-spleen SUV ratio for observers 1 and 2. The mean tumour-to-spleen SUV ratio of the high-grade tumours was greater than that of the low-grade tumours ($P=0.0003$ in observer 1, and $P=0.0029$ in observer 2)

Discussion

With the increased use of diagnostic imaging and improvements in imaging techniques, a greater number of RCCs are detected in asymptomatic patients [21, 22]. The appropriate treatment of RCC requires accurate diagnosis and characterization of each detected renal tumour. Although some characteristic imaging findings of cRCC are well known, including early enhancement, delayed wash-out, and the existence of a fatty component detected using in- and out-of-phase MR imaging [23–25], the preoperative estimation of biological grade remains uncertain, as there are no reliable radiological findings.

¹⁸F-FDG-PET/CT is a functional imaging modality for the detection of various malignant tumours on the basis of increased glucose uptake. Although the first indication of ¹⁸F-FDG-PET/CT for the detection of RCC was reported by Wahl et al. [26] in 1991, this technique is not commonly used for the detection of RCC, given the fact that the kidney is the major excretion route for ¹⁸F-FDG. Previous studies have demonstrated low sensitivity of ¹⁸F-FDG-PET/CT for the detection and diagnosis of RCC [27, 28]. Another clinical application of ¹⁸F-FDG-PET/CT is in estimating the biological grade of malignant tumours. Some studies have shown that increased uptake of ¹⁸F-FDG is observed more frequently in malignant tumours with higher pathological grades [29, 30].

Several systems have been proposed for the grading of RCCs. Nuclear grading systems have been shown to be more predictive of disease-specific survival in patients with RCC, regardless of pathologic stage [19, 31–37]. The Fuhrman system that classifies RCC into four grades according to nuclear size and the presence of nucleoli is currently the most widely

Table 4 Sensitivity, Specificity, and AUC for Differentiating Fuhrman Grades 3 and 4 Renal Clear Cell Carcinoma from Grades 1 and 2

	Tumor SUV _{max}		Tumor-to-Liver SUV ratio		Tumor-to-Spleen SUV ratio	
	Observer 1	Observer 2	Observer 1	Observer 2	Observer 1	Observer 2
Sensitivity	93 %	93 %	64 %	79 %	79 %	86 %
Specificity	59 %	59 %	100 %	88 %	82 %	65 %
AUC	0.76 (0.57–0.89)	0.76 (0.57–0.89)	0.82 (0.64–0.94)	0.83 (0.66–0.94)	0.80 (0.62–0.92)	0.75 (0.56–0.89)

AUC area under the ROC curve

used grading protocol in North America and Europe [31, 33, 38]. Since the introduction of this protocol, most studies have demonstrated significant disease-specific survival differences only after separating patients with Fuhrman grade 1 and 2 cRCCs from those with grade 3 and 4 tumours [14–18].

In our study, we used tumour-to-liver SUV and tumour-to-spleen SUV ratios in addition to tumour SUV_{max}. The liver and spleen were the representative organs with a high level of reticuloendothelial system activity. A previous report showed an increase in SUV_{mean} of the liver and spleen due to activation of a systemic immune response related to the presence of a viable malignant tumour [39]. In our results, liver and spleen SUVs demonstrated slightly lower values in high-grade tumours than in low-grade tumours, although there was no significant difference. Although the use of tumour SUV_{max} alone led to low specificity in the differentiation between Fuhrman grade 3/4 and grade 1/2 tumours due to considerable overlap between the two groups, tumour-to-liver and tumour-to-spleen SUV ratios showed high specificity (85–100 %), and cRCCs of high pathological grade were significantly associated with these increased values.

The use of tumour size as a predictive parameter for the malignant potential of RCC is controversial. One study found that the frequency of higher pathological grade in RCCs increased from 0 % for tumours smaller than 1 cm to 59 % for those larger than 7 cm [40]. However, most reports have indicated that tumour size alone is likely insufficient for predicting outcomes for patients with RCCs [41–43]. In the literature, some researchers have suggested a correlation between GLUT-1 receptor expression and pathological grade [12, 44]. Miyauchi et al. [45] found a positive correlation between GLUT-1 receptor expression and 18-F FDG uptake, and concluded that well-visualized RCCs on 18-F FDG-PET/CT are of a pathologically higher grade than those that are less well visualized. Their result is congruent with our study finding in which logistic regression analysis including tumour size as an independent factor demonstrated that tumour-to-liver SUV ratio was the only significant parameter for differentiating Fuhrman grade 3/4 tumours from others.

Our study had several limitations. First, it was retrospective in design, with a relatively small sample size. Further clinical studies with larger sample sizes may be necessary to validate

our preliminary results. Second, we evaluated only cRCCs, and an evaluation of other histological subtypes of RCCs may be warranted. Finally, the Fuhrman grading system was used as indicator of tumour aggressiveness. Other prognostic factors, including tumour size, retroperitoneal lymph nodes, adrenal involvement, and venous thrombi, may also contribute to the wide variability in outcomes that is seen in patients with cRCCs.

In summary, our study demonstrated a significant correlation between the tumour-to-liver SUV ratio and Fuhrman pathological grade. This ratio appears to be a valuable index for predicting pathological tumour grade in patients with cRCC. The use of 18-F FDG-PET/CT as an imaging biomarker may provide helpful information for clinical management in patients with cRCC.

Acknowledgments The scientific guarantor of this publication is Masayuki Kanematsu. The authors of this manuscript declare no relationships with any companies whose products or services may be related to the subject matter of the article. The authors state that this work has not received any funding. No complex statistical methods were necessary for this paper. Institutional review board approval was obtained. Written informed consent was obtained from all subjects (patients) in this study. Study subjects or cohorts have not been previously reported. Methodology: retrospective diagnostic multicenter study.

References

1. Siegel R, Naishadham D, Jemal A (2012) Cancer statistics, 2012. *CA Cancer J Clin* 62:10–29
2. Leibovich BC, Lohse CM, Crispen PL et al (2010) Histological subtype is an independent predictor of outcome for patients with renal cell carcinoma. *J Urol* 183:1309–1315
3. Teloken PE, Thompson RH, Tickoo SK et al (2009) Prognostic impact of histological subtype on surgically treated localized renal cell carcinoma. *J Urol* 182:2132–2136
4. Luciani LG, Cestari R, Tallarigo C (2000) Incidental renal cell carcinoma—Age and stage characterization and clinical implications: study of 1092 patients (1982–1997). *Urology* 56:58–62
5. Jayson M, Sanders H (1998) Increased incidence of serendipitously discovered renal cell carcinoma. *Urology* 51:203–205
6. Hustinx R, Benard F, Alavi A (2002) Whole-body FDG-PET imaging in the management of patients with cancer. *Semin Nucl Med* 32:35–46

7. Scott AM (2001) Current status of positron emission tomography in oncology. *Intern Med J* 31:27–36
8. Flier JS, Mueckler MM, Usher P, Lodish HF (1987) Elevated levels of glucose transport and transporter messenger RNA are induced by ras or src oncogenes. *Science* 235:1492–1495
9. Monakhov NK, Neistadt EL, Shavlovskil MM, Shvartsman AL, Neifakh SA (1978) Physicochemical properties and isoenzyme composition of hexokinase from normal and malignant human tissues. *J Natl Cancer Inst* 61:27–34
10. Miyakita H, Tokunaga M, Onda H et al (2002) Significance of ¹⁸F-fluorodeoxyglucose positron emission tomography (FDG-PET) for detection of renal cell carcinoma and immunohistochemical glucose transporter 1 (GLUT-1) expression in the cancer. *Int J Urol* 9:15–18
11. Ramdave S, Thomas GW, Berlangieri SU et al (2001) Clinical role of ¹⁸F-fluorodeoxyglucose positron emission tomography for detection and management of renal cell carcinoma. *J Urol* 166:825–830
12. Aide N, Cappelletti O, Bottet P et al (2003) Efficiency of [¹⁸F]FDG PET in characterising renal cancer and detecting distant metastases: a comparison with CT. *Eur J Nucl Med Mol Imaging* 30:1236–1245
13. Kang DE, White RL, Zuger JH, Sasser HC, Teigland CM (2004) Clinical use of fluorodeoxyglucose F 18 positron emission tomography for detection of renal cell carcinoma. *J Urol* 171:1806–1809
14. Medeiros LJ, Gelb AB, Weiss LM (1988) Renal cell carcinoma. Prognostic significance of morphologic parameters in 121 cases. *Cancer* 61:1639–1651
15. Grignon DJ, Ayala AG, el-Naggar A et al (1989) Renal cell carcinoma. A clinicopathologic and DNA flow cytometric analysis of 103 cases. *Cancer* 64:2133–2140
16. Munichor M, Lichtig C, Tzin G, Weiss A (1992) Prognostic significance of granular cell content in renal cell carcinoma. *Eur Urol* 22:204–208
17. Bretheau D, Lechevallier E, de Fromont M, Sault MC, Rampal M, Coulange C (1995) Prognostic value of nuclear grade of renal cell carcinoma. *Cancer* 76:2543–2549
18. Usbutun A, Uygur MC, Ayhan A et al (1998) Comparison of grading systems for estimating the prognosis of renal cell carcinoma. *Int Urol Nephrol* 30:391–397
19. Frank I, Blute ML, Cheville JC, Lohse CM, Weaver AL, Zincke H (2002) An outcome prediction model for patients with clear cell renal cell carcinoma treated with radical nephrectomy based on tumor stage, size, grade and necrosis: the SSIGN score. *J Urol* 168:2395–2400
20. Hanley JA, McNeil BJ (1983) A method of comparing the areas under receiver operating characteristic curves derived from the same cases. *Radiology* 148:839–843
21. Mathew A, Devesa SS, Fraumeni JF, Chow WH (2002) Global increases in kidney cancer incidence, 1973–1992. *Eur J Cancer Prev* 11:171–178
22. Volpe A, Jewett MAS, Evans AJ (2004) The natural history of incidentally detected small renal masses – Author reply. *Cancer* 101:651–652
23. Sheir KZ, El-Azab M, Mosbah A, El-Baz M, Shaaban AA (2005) Differentiation of renal cell carcinoma subtypes by multislice computerized tomography. *J Urol* 174:451–455, discussion 455
24. Ruppert-Kohlmayr AJ, Uggowitz M, Meissnitzer T, Ruppert G (2004) Differentiation of renal clear cell carcinoma and renal papillary carcinoma using quantitative CT enhancement parameters. *AJR Am J Roentgenol* 183:1387–1391
25. Outwater EK, Bhatia M, Siegelman ES, Burke MA, Mitchell DG (1997) Lipid in renal clear cell carcinoma: detection on opposed-phase gradient-echo MR images. *Radiology* 205:103–107
26. Wahl RL, Hamey J, Hutchins G, Grossman HB (1991) Imaging of renal-cancer using positron emission tomography with 2-deoxy-2(18f)-fluoro-D-glucose – pilot animal and human studies. *J Urol* 146:1470–1474
27. Kocher F, Grimm S, Hautmann R, Reske SN (1994) Preoperative lymph-node staging in patients with kidney and urinary-bladder neoplasm. *J Nucl Med* 35:P223–P224
28. Ozulker T, Ozulker F, Ozbek E, Ozpacaci T (2011) A prospective diagnostic accuracy study of ¹⁸F-fluorodeoxyglucose-positron emission tomography/computed tomography in the evaluation of indeterminate renal masses. *Nucl Med Commun* 32:265–272
29. Lippitz B, Cremerius U, Mayfrank L et al (1996) PET-study of intracranial meningiomas: correlation with histopathology, cellularity and proliferation rate. *Acta Neurochir Suppl* 65:108–111
30. Nakajo M, Kajiya Y, Kaneko T et al (2010) FDG PET/CT and diffusion-weighted imaging for breast cancer: prognostic value of maximum standardized uptake values and apparent diffusion coefficient values of the primary lesion. *Eur J Nucl Med Mol Imaging* 37:2011–2020
31. Fuhrman SA, Lasky LC, Limas C (1982) Prognostic significance of morphologic parameters in renal cell carcinoma. *Am J Surg Pathol* 6:655–663
32. Thoenes W, Storkel S, Rumpelt HJ (1986) Histopathology and classification of renal cell tumors (adenomas, oncocytomas and carcinomas). The basic cytological and histopathological elements and their use for diagnostics. *Pathol Res Pract* 181:125–143
33. Medeiros LJ, Jones EC, Aizawa S et al (1997) Grading of renal cell carcinoma – Workgroup no 2. *Cancer* 80:990–991
34. Mejean A, Oudard S, Thiounn N (2003) Prognostic factors of renal cell carcinoma. *J Urol* 169:821–827
35. Patard JJ, Leray E, Rodriguez A, Rioux-Leclercq N, Guille F, Lobel B (2003) Correlation between symptom graduation, tumor characteristics and survival in renal cell carcinoma. *Eur Urol* 44:226–232
36. Tsui KH, Shvarts O, Smith RB, Figlin RA, deKernion JB, Belldgrun A (2000) Prognostic indicators for renal cell carcinoma: a multivariate analysis of 643 patients using the revised 1997 TNM staging criteria. *J Urol* 163:1090–1095
37. Ficarra V, Prayer-Galetti T, Novella G et al (2003) Incidental detection beyond pathological factors as prognostic predictor of renal cell carcinoma. *Eur Urol* 43:663–669
38. Bostwick DG, Murphy GP (1998) Diagnosis and prognosis of renal cell carcinoma: highlights from an international consensus workshop. *Semin Urol Oncol* 16:46–52
39. Bural GG, Torigian DA, Chen W, Houseni M, Basu S, Alavi A (2010) Increased ¹⁸F-FDG uptake within the reticuloendothelial system in patients with active lung cancer on PET imaging may indicate activation of the systemic immune response. *Hell J Nucl Med* 13:23–25
40. Thompson RH, Kurta JM, Kaag M et al (2009) Tumor size is associated with malignant potential in renal cell carcinoma cases. *J Urol* 181:2033–2036
41. Crispin PL, Wong YN, Greenberg RE, Chen DYT, Uzzo RG (2008) Predicting growth of solid renal masses under active surveillance. *Urol Oncol* 26:555–559
42. Hsu RM, Chan DY, Siegelman SS (2004) Small renal cell carcinomas: correlation of size with tumor stage, nuclear grade, and histologic subtype. *AJR Am J Roentgenol* 182:551–557
43. Delahunt B, Bethwaite PB, Nacey JN (2007) Outcome prediction for renal cell carcinoma: evaluation of prognostic factors for tumours divided according to histological subtype. *Pathology* 39:459–465
44. Montravers F, Grahek D, Kerrou K et al (2000) Evaluation of FDG uptake by renal malignancies (primary tumor or metastases) using a coincidence detection gamma camera. *J Nucl Med* 41:78–84
45. Miyauchi T, Brown RS, Grossman HB, Wojno K, Wahl RL (1996) Correlation between visualization of primary renal cancer by FDG-PET and histopathological findings. *J Nucl Med* 37:245–245